Electronic Supplementary Material (ESI) for Journal of Materials Chemistry A.

Electronic Supplementary Information (ESI)

Stable electron-deficient metal-organic framework for colorimetric and luminescent sensing of phenols and anilines

Teng Gong,[a] *Peng Li,*[a] *Qi Sui,*[a] *Jinquan Chen,*[b] *Jianhua Xu*[b] *and En-Qing Gao*[a]*

[a] Shanghai Key Laboratory of Green Chemistry and Chemical Processes, School of Chemistry and Molecular Engineering, East China Normal University, Shanghai 200062,P. R. China
E-mail: eqgao@chem.ecnu.edu.cn
[b] State Key Laboratory of Precision Spectroscopy, East China Normal University,Shanghai 200062, P. R. China

Experimental

Physical methods. ^{1}H NMR spectra were recorded on a Bruker Advance 400 MHz spectrometer. FT-IR spectra were recorded in the range 500 - 4000 cm-1 using KBr pellets on a Nicolet NEXUS 670 spectrophotometer. Elemental analyses were determined on an Elementar Vario ELIII analyzer. Powder X-ray diffraction (PXRD) was recorded on a Rigaku Ultima IV X-ray diffractometer equipped with a Cu-target tube at 35 kV, 25 mA and a graphite monochromator. Thermogravimetric (TG) analysis was performed with a STA 449 F3 Simultaneous Thermal Analyzer in the temperature range from 25 to 800 ℃ in flowing air with a heating rate of 10 ℃/min. Scanning electron microscopy (SEM) and EDX measurements were taken on an S-4800 (HITACHI, Japan) operating at 10 kV, 100 μA. Nitrogen adsorption and desorption isotherm measurements were performed on a Micromeritics ASAP2020 analyzer at 77 K and the sample was activated at 100 °C for 4 h under dynamic vacuum before measurements. Luminescence spectra were recorded on a FluoroMax-4 fluorescence spectrometer either with ground solid samples or with dispersions (0.75 mg/mL in water unless specified otherwise) obtained by sonication.

X-ray crystallography. Data collection for **LVMOF-1** was measured at 150 K on a Bruker D8 VENYURE diffractometer equipped with a CCD area detector and graphite-monochromated Cu Kα radiation (λ = 1.54178 Å). Data collection for **aniline@LVMOF-1** was conducted at 296 K using a Bruker APEX II diffractometer (Mo Kα radiation, λ = 0.71073 Å) equipped with a graphite-monochromated and a CCD area detector. The structures were solved by direct methods and refined by the full-matrix least-squares method on F^2, with all non-hydrogen atoms refined with anisotropic displacement parameters.[1] All hydrogen atoms attached to carbons were calculated geometrically and refined using the riding model. In the structures, the viologen moiety is disordered over two equivalent sites related by the crystallographic 2-fold axis. The anions are also disordered. The guest solvent molecules were highly disordered, which could not be modeled as discrete atomic sites. Contributions of these solvent molecules of **LVMOF-1** to scattering were removed using the SQUEEZE routine of PLATON. A summary of the crystallographic data, data collection, and refinement parameters are provided in Table S1. Note: the reported formula includes 8 guest water molecules, which was estimated according to analytic results. This causes a level A alert in checkCIF report.

Table S1. Crystallographic Data and Structure Refinements Parameters for **LVMOF-1** and **aniline@LVMOF-1**.

	LVMOF-1	**Aniline@LVMOF-1**
Empirical formula	$C_{28}H_{40}N_2O_{20}Cl_2Eu_2$	$C_{34}H_{37}N_3O_{15}Cl_2Eu_2$
Formula weight	1099.44	1102.48
Crystal system	Orthorhombic	Orthorhombic
Space group	*Ima2*	*Ima2*
a, Å	9.7764(5)	9.7765(4)
b, Å	28.1748(14)	28.3415(11)
c, Å	7.1892(4)	7.1889(3)
α, deg	90	90
β, deg	90	90
γ, deg	90	90
V, Å^3	1980.25(18)	1991.90(14)
Z	2	2
ρ_{calcd}, g cm^{-3}	1.844	1.838
μ, mm^{-1}	24.386	3.325
θ range collected	4.788 – 68.218	1.437 – 28.368
Data / unique	4222 / 1467	9640 / 2370
R_{int}	0.0445	0.0242
S on F^2	0.996	1.086
R_1, wR_2 [$I > 2\sigma(I)$]	0.0668, 0.1818	0.0257, 0.0758
R_1, wR_2 (all data)	0.0671, 0.1825	0.0274, 0.0770

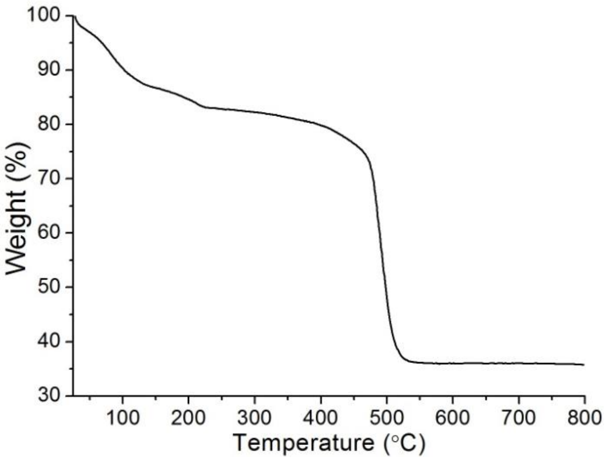

Fig. S1. TG curve of **LVMOF-1**.

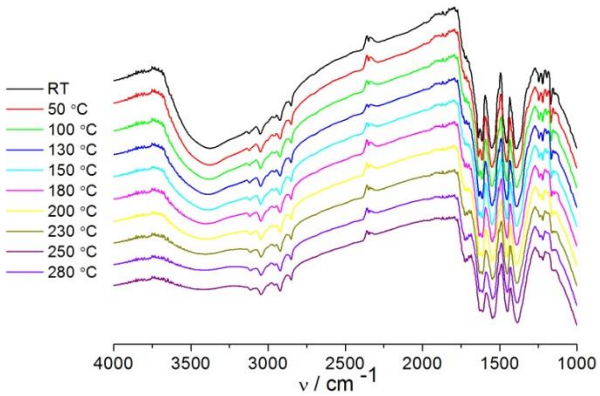

Fig. S2. *In situ* temperature-dependent IR spectra of **LVMOF-1** in vacuum.

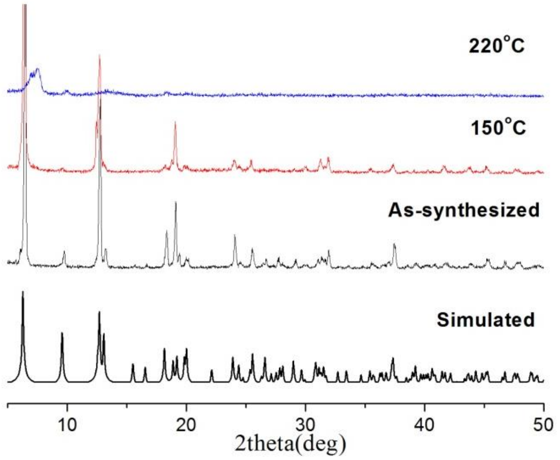

Fig. S3. PXRD patterns of **LVMOF-1** at different temperatures.

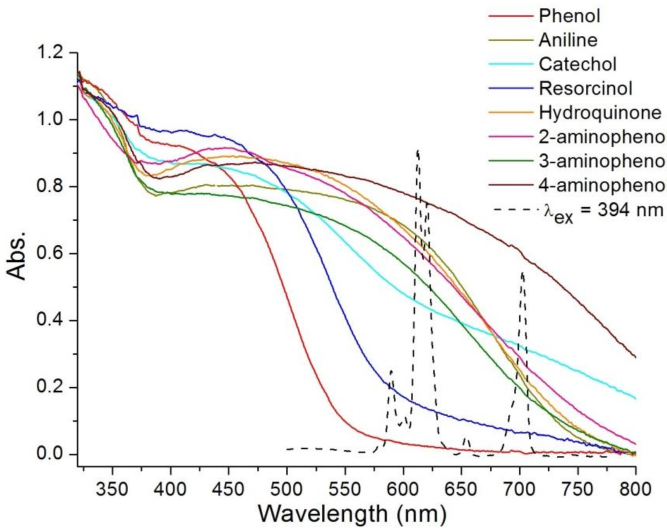

Fig. S4. UV-vis spectra of **LVMOF-1** after adsorbing different electron-rich aromatics. The emission spectrum of pristine **LVMOF-1** (excited at 394 nm) is also given to show its overlap with the CT band after guest inclusion.

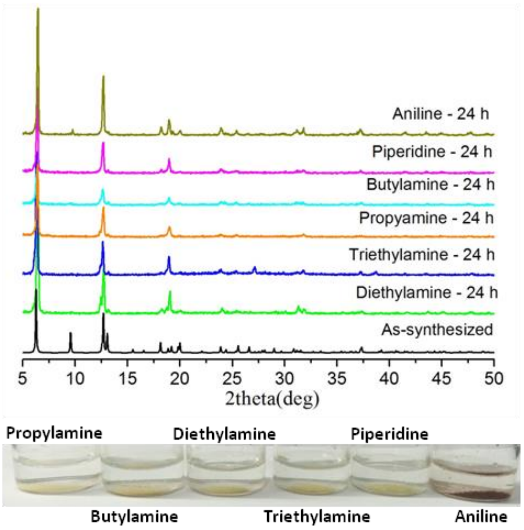

Fig. S5. PXRD (top) and photographs (bottom) of **LVMOF-1** after treated by different organic amines. Only aniline causes appreciable color change of the MOF.

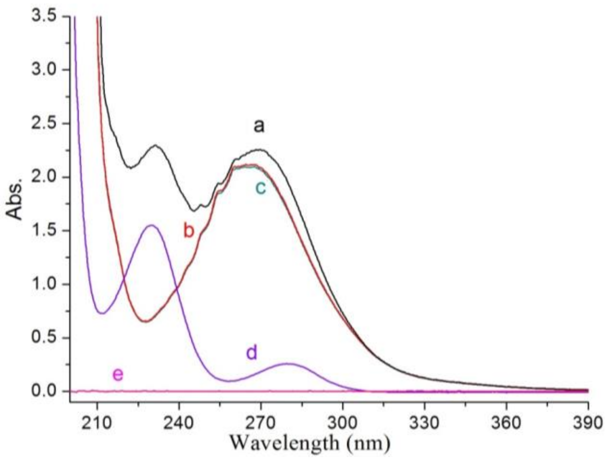

Fig. S6. UV-vis spectra showing the selective absorption of aniline against benzene and nitrobenezene. (a) The spectrum for a mixed aqueous solution containing 0.5 mM aniline, 0.64 mM benzene and 0.0075 mM nitrobenzene. (b) The spectrum for the mixed solution treated with excessive **LVMOF-1** (4 mL of the mixed solution was stirred with 10 mg of the MOF at room temperature for 24 h, and the spectrum was measured with the supernatant obtained by centrifugation). (c) The spectrum for an aqueous solution containing 0.64 mM benzene and 0.0075 mM nitrobenzene. *The superposition between (b) and (c) indicates that aniline was almost completed removed while benzene and nitrobenzene were hardly absorbed.* (d) The spectrum for an aqueous solution of aniline (0.5 mM). (e) The spectrum for the aniline solution treated with excessive **LVMOF-1** by the procedure described for the mixed solution (b). This spectrum confirms that aniline is completely removed with respect to the detection limit of the UV spectrometry.

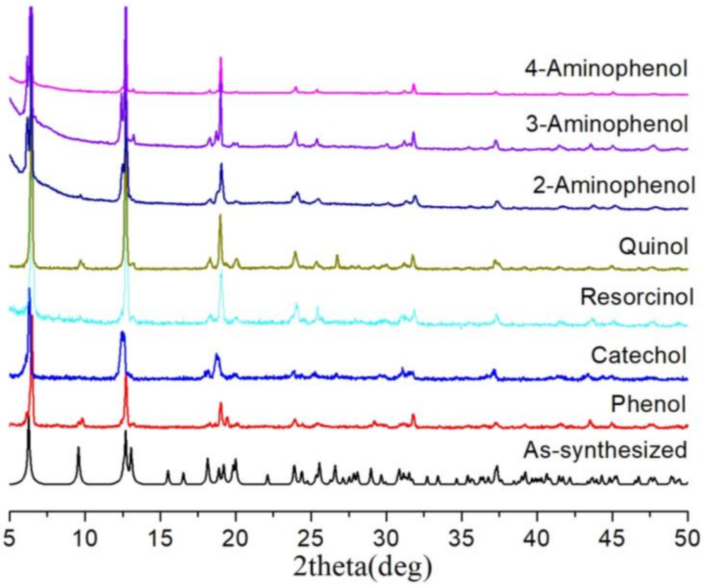

Fig. S7. PXRD of **LVMOF-1** after exchange with different anions and absorption of different electron-rich aromatics.

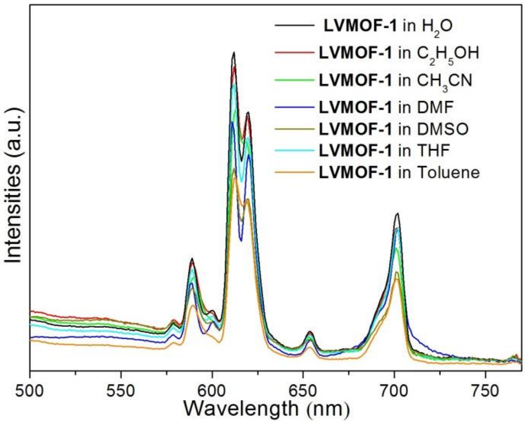

Fig. S8. Photoluminescent spectra of **LVMOF-1** dispersed in different solvents excited at 394 nm.

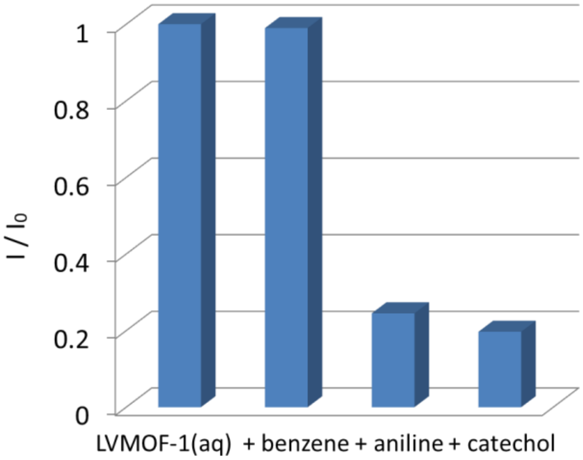

Fig.S9. Relative intensity for the $^5D_0 \rightarrow ^7F_2$ emission of the LVMOF-1 aqueous dispersion as benzene, aniline and catechol were *successively* added. The concentration of each analyte is 0.1 mM. This test confirms that MOF shows selective response to electron donating aromatics in mixed systems and that two coexistent donor analytes causes stronger quenching than a single analyte.

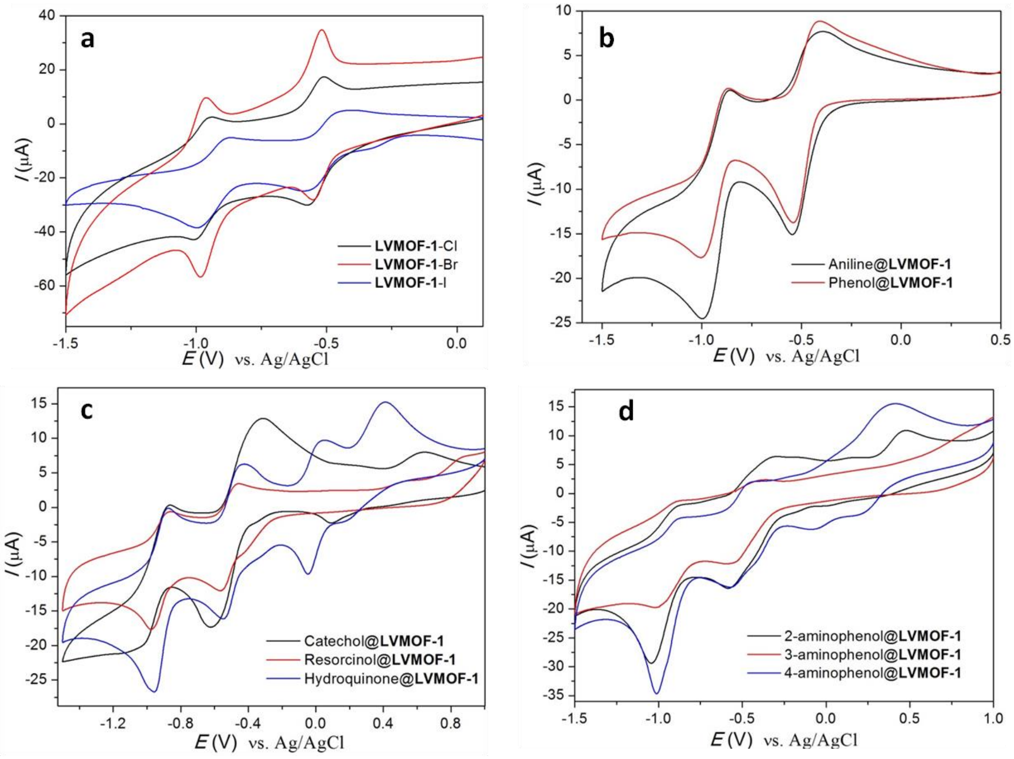

Fig. S10. Cyclic voltammograms of **LVMOF-1-X** (a. X = Cl$^-$, Br$^-$, and I$^-$) and electron-rich **aromatics@LVMOF-1** (b, c, d).

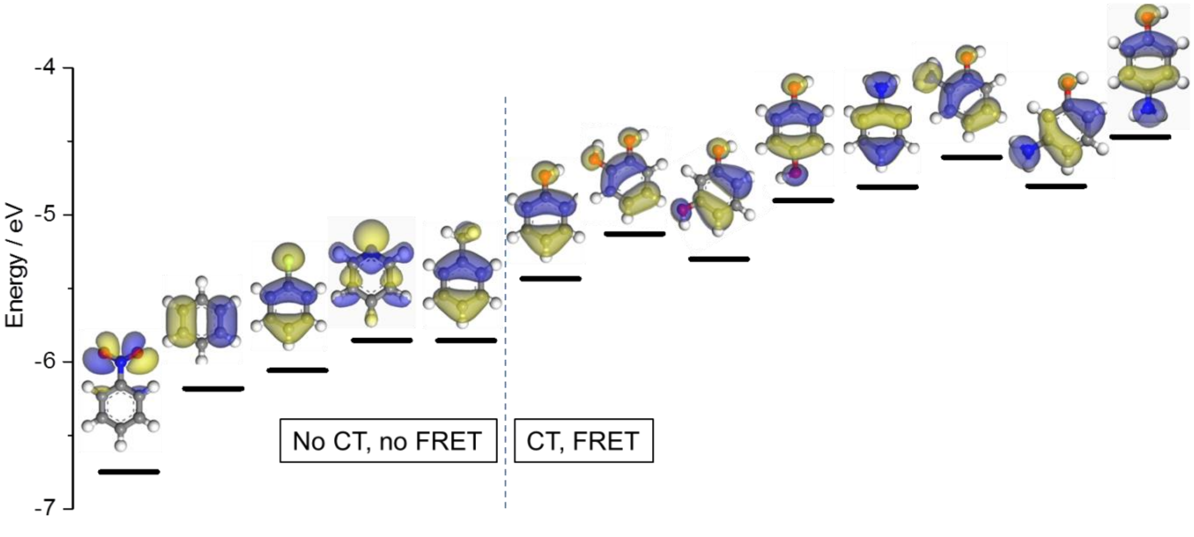

Fig. S11. Comparison of the HOMOs of different aromatic compounds..

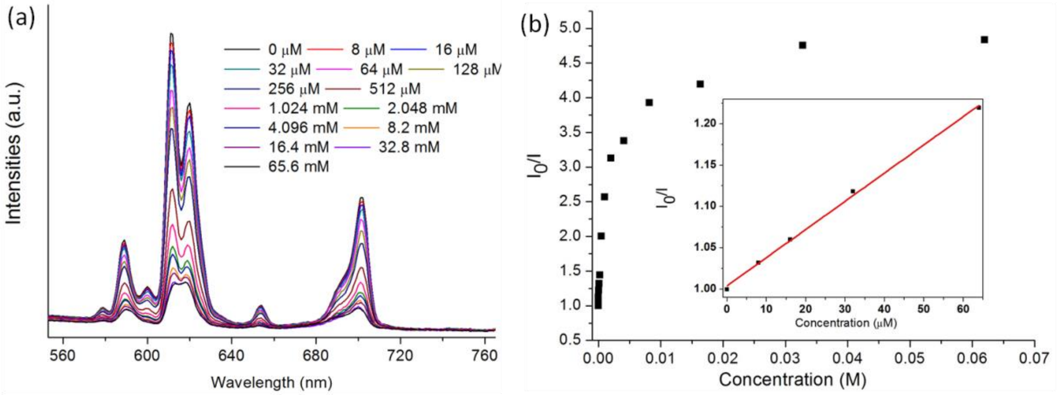

Fig. S12. (a) Emission spectra of the **LVMOF-1** aqueaous dispersion with the incremental addition of phenol in aqueous solution (the phenol concentrations are labeled). (b) Stern−Volmer curve acquired from the $^5D_0 \rightarrow {}^7F_2$ transition. Inset: Stern−Volmer fit in the low concentration region.

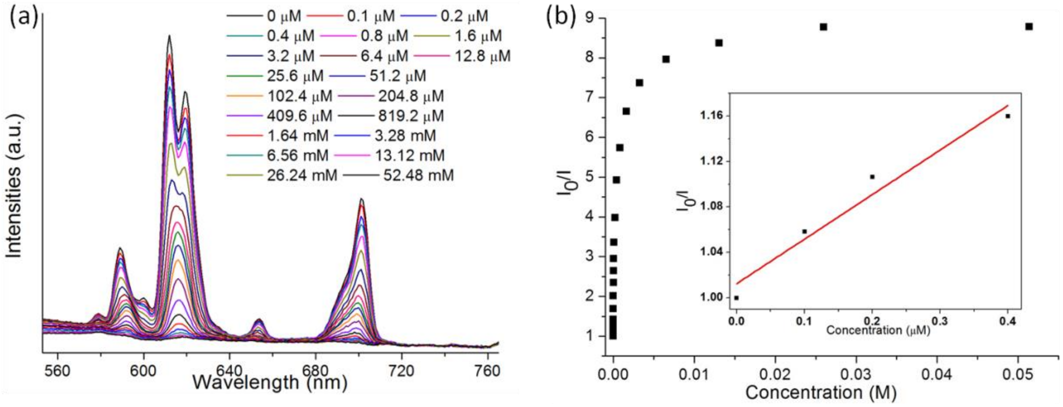

Fig. S13. (a) Emission spectra of the **LVMOF-1** aqueaous dispersion with the incremental addition of catechol in aqueous solution (the catechol concentrations are labeled). (b) Stern−Volmer curve acquired from the $^5D_0 \rightarrow {}^7F_2$ transition. Inset: Stern−Volmer fit in the low concentration region.

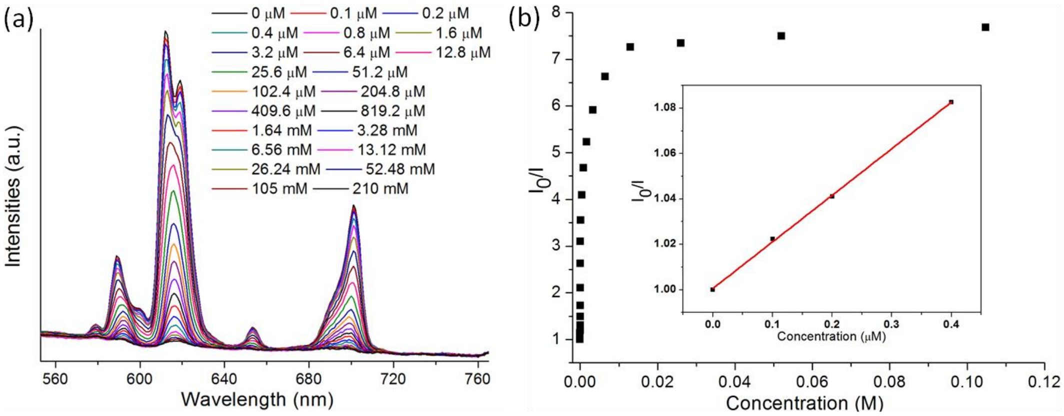

Fig. S14. (a) Emission spectra of the **LVMOF-1** aqueaous dispersion with the incremental addition of resorcinol in aqueous solution (the resorcinol concentrations are labeled). (b) Stern−Volmer curve acquired from the $^5D_0 \rightarrow {}^7F_2$ transition. Inset: Stern−Volmer fit in the low concentration region.

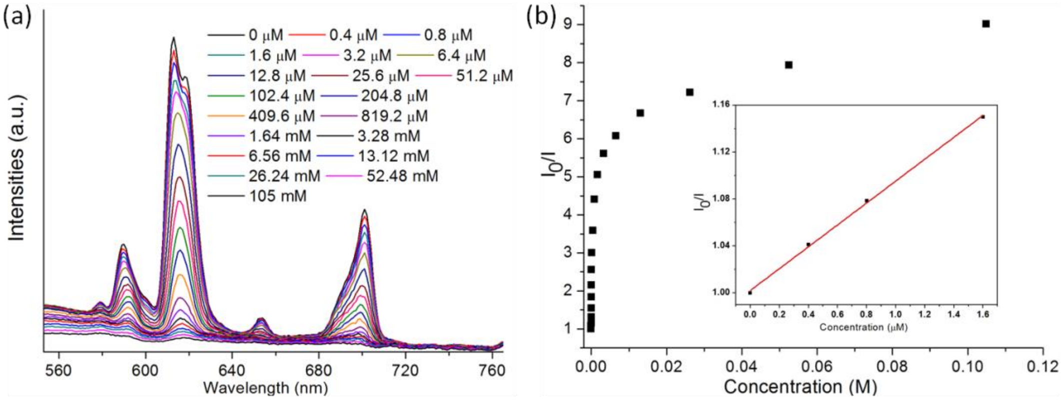

Fig. S15. (a) Emission spectra of the **LVMOF-1** aqueaous dispersion with the incremental addition of hydroquinone in aqueous solution (the hydroquinone concentrations are labeled). (b) Stern−Volmer curve acquired from the $^5D_0 \rightarrow {}^7F_2$ transition. Inset: Stern−Volmer fit in the low concentration region.

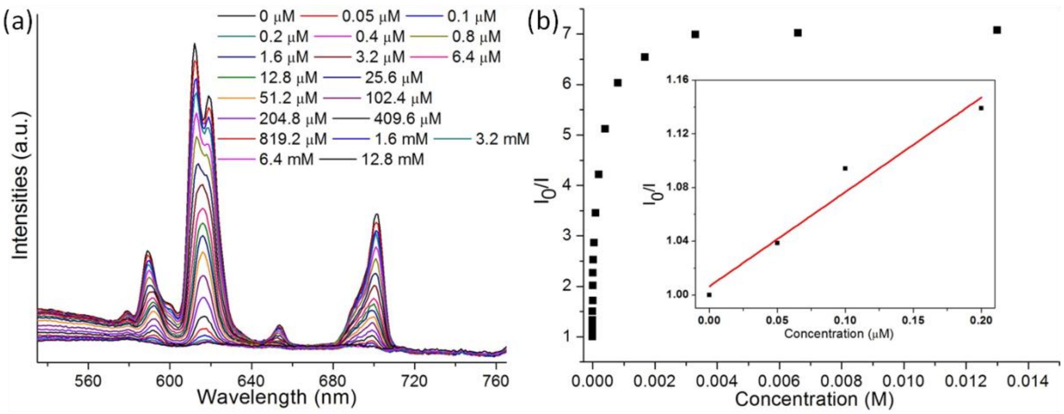

Fig. S16. (a) Emission spectra of the **LVMOF-1** aqueaous dispersion with the incremental addition of 2-aminophenol in aqueous solution (the 2-aminophenol concentrations are labeled). (b) Stern−Volmer curve acquired from the $^5D_0 \rightarrow ^7F_2$ transition. Inset: Stern−Volmer fit in the low concentration region.

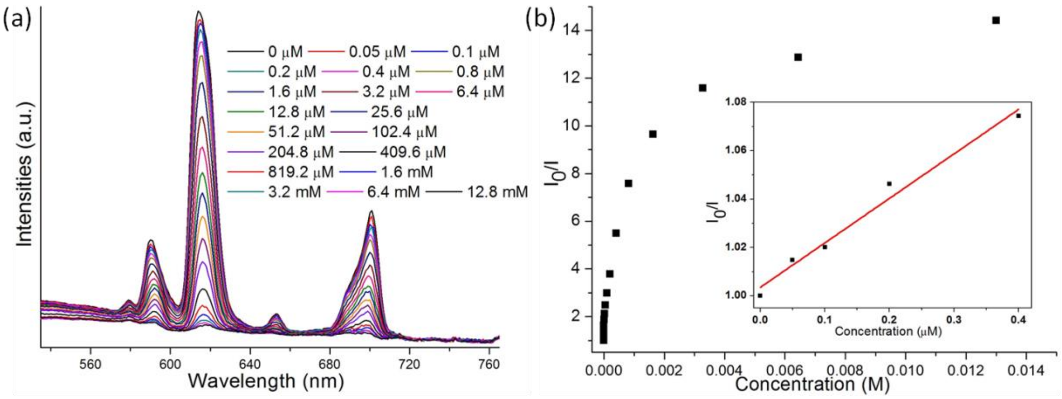

Fig. S17. (a) Emission spectra of the **LVMOF-1** aqueaous dispersion with the incremental addition of 3-aminophenol in aqueous solution (the 3-aminophenol concentrations are labeled). (b) Stern−Volmer curve acquired from the $^5D_0 \rightarrow ^7F_2$ transition. Inset: Stern−Volmer fit in the low concentration region.

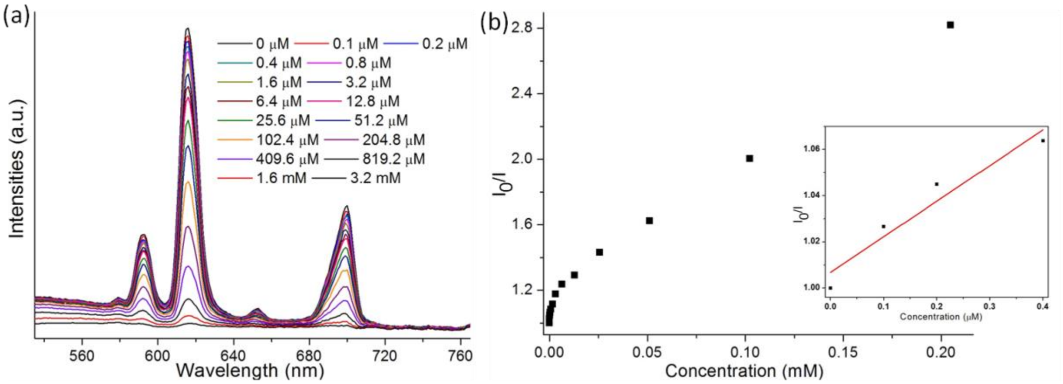

Fig. S18. (a) Emission spectra of the **LVMOF-1** aqueaous dispersion with the incremental addition of 4-aminophenol in aqueous solution (the 4-aminophenol concentrations are labeled). (b) Stern−Volmer curve acquired from the $^5D_0 \rightarrow ^7F_2$ transition. Inset: Stern−Volmer fit in the low concentration region.

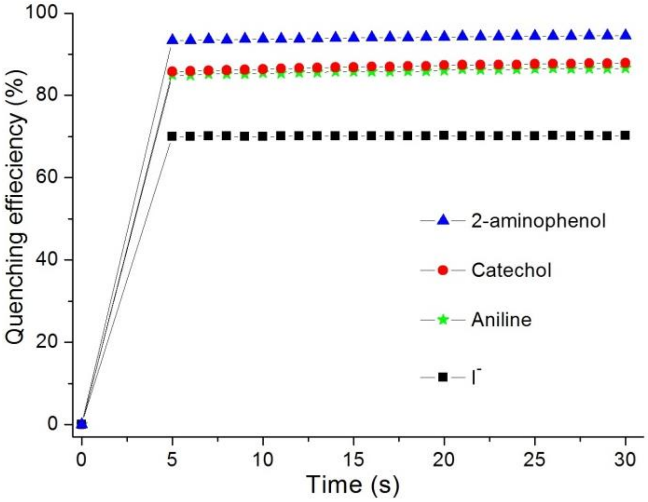

Fig. S19. Time dependence of the quenching effieciency [(1-I/I$_0$)×100%] at 614 nm (excited at 394 nm) of the aqueous dispersions of **LVMOF-1** upon addition of I$^-$, aniline, catechol and 2-aminophenol (1.0 mM).

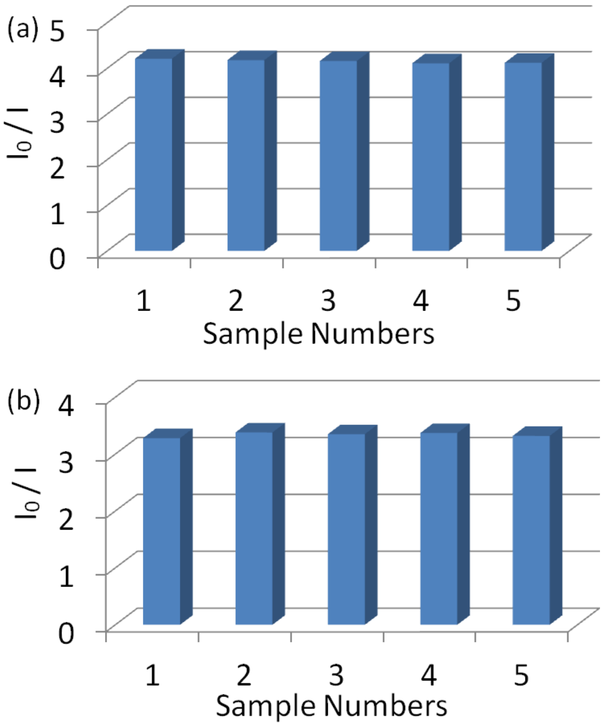

Fig. S20. Comparison of I_0/I for parallel experiments with aniline (a) and catechol (b). I_0/I is the intensity ratio of the $^5D_0 \rightarrow {}^7F_2$ emission detected before and after the analyte was added to a LVMOF-1/water dispersion. The concentration of the analyte is 0.1 mM..

Table S2. Detection limits (DL) of luminescence sensors for detection of phenols and anilines

Analyte	Probe / sensor	*DL* (μM)	*Ref*
Aniline	Eu-BDC-MOF-1	6.8	[2]
Aniline	Eu-BDC-MOF-2	9.0	[2]
Aniline	Green fluorescence protein	0.01	[3]
Aniline	metallo-tetraazaporphyrin dye	0.11	[4]
Catechol	$[C_3(AmP)_2][OH]_2$	0.4	[5]
Hydroquinone	$[C_3(AmP)_2][OH]_2$	0.31	[5]
Hydroquinone	carbon dots	0.1	[6]
Hydroquinone	CdTe QDs- enzyme	0.5	[7]
Hydroquinone	CP $PPESO_3$-enzyme	0.5	[8]

References

1. G. Sheldrick, *Bruker Analytical X-ray Instruments Inc., Madison, Wisconsin, USA*, 1998.

2. H.-J. Feng, L. Xu, B. Liu and H. Jiao, *Dalton Trans.*, 2016, **45**, 17392-17400.
3. A. S. Vangnai, N. Kataoka, S. Soonglerdsongpha, C. Kalambaheti, T. Tajima and J. Kato, *J. Ind. Microbiol. Biotechnol.*, 2012, **39**, 1801-1810.
4. R. Prasad, R. Kumar and S. Prasad, *Anal. Chim. Acta*, 2009, **646**, 97-103.
5. S. K. Patil, S. A. Patil, M. M. Vadiyar, D. V. Awale, A. S. Sartape, L. S. Walekar, G. B. Kolekar, U. V. Ghorpade, J. H. Kim and S. S. Kolekar, *J.Mol. Liq.*, 2017, **244**, 39-45.
6. P. Ni, H. Dai, Z. Li, Y. Sun, J. Hu, S. Jiang, Y. Wang and Z. Li, *Talanta*, 2015, **144**, 258-262.
7. J. Yuan, W. Guo and E. Wang, *Anal. Chem.*, 2008, **80**, 1141-1145.
8. H. Huang, M. Xu, Y. Gao, G. Wang and X. Su, *Talanta*, 2011, **86**, 164-169.